Lassa virus NP DEDDh 3'-5' exoribonuclease activity is required for optimal viral RNA replication.

Cheng Huang[1]*, Emily Mantlo[1,2,] Slobodan Paessler[1],

[1]Department of Pathology, Galveston National Laboratory and Institute for Human Infections and Immunity, University of Texas Medical Branch, Galveston, TX, USA

[2] Current address: Department of Diagnostic Medicine/Pathobiology, College of Veterinary Medicine, Kansas State University, Manhattan, Kansas, USA.

*Corresponding Author: Cheng Huang, chhuang@utmb.edu Tel: 409-266-6934

Abstract

Mammarenavirus include several pathogens that can cause severe and fatal zoonotic diseases in humans. Lassa virus (LASV) is the causative agent for Lassa fever (LF) currently endemic in West Africa. There is no approved vaccines and antivirals against LASV infection. Despite the substantial threat of LASV to public health, important questions in the basic biology of LASV still exist. LASV nucleoprotein has a DEDDH 3'-to-5' exoribonuclease motif (ExoN), which is known to degrade virus-derived double-stranded RNA and thereby is key to LASV evasion of interferon response. Intriguingly, the NP ExoN motif is highly conserved in mammarenaviruses, regardless of pathogenicity, suggesting that NP ExoN has important function in virus life cycle in addition to immune evasion. By using reverse genetics system, we rescued an ExoN-deficient LASV mutant (ExoN- rLASV). Compared to wild-type rLASV, the ExoN- rLASV demonstrated impaired virus growth and decreased viral RNA production in interferon-deficient cells. For the first time, we found that abrogation of LASV ExoN activity led to increased aberrant viral RNA production in infection. Furthermore, NP ExoN deficiency increased LASV sensitivity to mutagenic nucleoside analogue. Our study provided evidence for an additional role of LASV NP ExoN in viral RNA replication besides its recognized function in immune evasion. LASV ExoN activity may be required for optimal viral RNA synthesis and control of aberrant viral RNA and viral RNA mutation.

Significance

LASV NP contains a DEDDh ExoN motif, through which LASV is capable of degrading virus-derived, immunostimulatory dsRNA to eliminate the danger signal and inhibit interferon response. Intriguingly, the NP ExoN motif is highly conserved among

arenavirus family, regardless of pathogenicity and viral capability to suppress host innate immune response. Therefore, arenavirus NP ExoN may have yet-to-be-identified function in virus infection. In this study, we discovered that abrogation of LASV NP ExoN activity impaired viral RNA replication in interferon-deficient cells and enhanced virus sensitivity to mutagenic nucleoside analogue. Our new findings indicate that LASV NP ExoN participates in optimal viral RNA replication and open new directions for future studies. Elucidating the function of LASV NP ExoN may promote our understanding of the basics of LASV replication and inform antiviral and vaccine development.

Introduction

Arenaviridae consists of four genera, *Mammarenavirus*, *Reptarenavirus*, *Hartmanivirus*, and *Antennavirus (1, 2)*. Mammarenviruses (referred to as arenavirus hereafter) include several pathogens of major clinical importance. These arenaviruses mainly infect their rodent hosts, often persistently without causing overt disease signs. Spillover to humans could occur through aerosol inhalation leading to severe or fatal zoonotic diseases (3-6). The Old World Lassa virus (LASV) causes Lassa fever (LF) with sever morbidity and high case fatality and is endemic in West Africa (7). The recent LF outbreaks in Nigeria featured high fatality rates of up to 25.4% (8, 9). LF is also associated with a high incidence of sequelae: approximately one-third of LF survivors suffer from sudden-onset sensorineural hearing loss, which constitutes a neglected public health and social burden (10). The New World arenavirus Junín virus (JUNV) and Machupo virus (MACV) sporadically cause Argentine hemorrhagic fever (AHF) and Bolivian hemorrhagic fever (BHF) in South America (4, 11, 12). Vaccines and

treatments are limited for these highly pathogenic arenaviruses. Accordingly, LASV, JUNV and MACV are classified as Category A Priority Pathogens in the USA. The World Health Organization has listed LF in the Blueprint list of priority diseases for which there is an urgent need for accelerated research and development (13).

Arenaviruses are negative-sense RNA virus with a single-stranded, bi-segmented RNA genome. The large (L) segment genomic RNA (L gRNA) and the small (S) segment genomic RNA (S gRNA) is around 7.2 kb and 3.4 kb, respectively, in length (Fig 1A). Each genomic RNA contains two coding regions separated by a highly structured, GC-rich intergenic region (IGR) (Fig 1A). The L segment encodes the RNA-dependent RNA polymerase (RdRp) L protein and a small, zinc finger protein (Z), which drives the assembly and budding of virus particles. The S segment encodes the viral glycoprotein (GP), which mediates virus entry, and the nucleoprotein (NP), which is the major structural component of the nucleocapsid (14). L protein and NP are both required for viral RNA replication (15) in virus-induced, discrete cytosolic structures (16). After virus entry, NP mRNA and L mRNA are first synthesized from S gRNA and L gRNA, respectively. mRNA transcription is terminated at IGR, which is the bona fade termination signal (Fig 1B). Arenavirus mRNA lacks a poly-A tail that is essential for the stability of conventional mRNA in host cells. Histone and HCV mRNAs, which also lack the poly-A tail, are stabilized by stem-loop structures at 3’-ends (17, 18). It is believed that arenavirus mRNA could be stabilized by IGR element at the 3’-end in a similar manner. Anti-genomic S RNA (S agRNA) and anti-genomic L RNA (L agRNA) are also synthesized from S gRNA and L gRNA. Later in infection, GPC mRNA and Z mRNA are transcribed from S agRNA and L agRNA, respectively (Fig 1B). Of note, IGR element is

also required for efficient incorporation of arenavirus genomic RNA into progeny virus particles (19).

Arenavirus NP contains two structurally and functionally separated domains. The N-terminal half (aa 1-340 in LASV NP) binds to viral genomic RNA to form vRNP (20). In the C-terminal half of LASV NP, residues D389, E391, D466, D533 and H528 constitute a DEDDh 3'-5' exoribonuclease (ExoN)-like motif. Structural and biochemical studies have experimentally proved that LASV NP DEDDh motif harbors exoribonuclease activity specificity for double-stranded RNA (dsRNA). Mutation of any of these critical residues abolishes the ExoN activity (21-23). These studies have also revealed ExoN activity is essential for LASV NP inhibition of Sendai virus-induced interferon response (21, 23), which is in line with LASV suppression of innate immune response *in vitro* and *in vivo*. RNA virus replication often generates dsRNA products, which can be sensed by host Pattern Recognition Receptors (RIG-I, MDA5 and PKR etc.) and trigger signaling cascades that lead to an anti-viral innate immune response mediated by IFN/cytokines. Thus, the LASV NP ExoN activity to degrade virus-derived dsRNA is believed key to LASV immune evasion and pathogenicity (24, 25).

Interestingly, the NP DEDDh motif and its 3'-5' ExoN activity are highly conserved in arenaviruses regardless of pathogenicity. For instance, NPs of non-pathogenic arenavirus Tacaribe virus (TCRV), Pichinde virus (PICV) and Mopeia virus (MOPV) also have the ExoN activity (22, 26-28). In addition, arenaviral NP ExoN activity is not correlated with viral capability to suppress IFN response. MOPV and TCRV infection stimulate IFN and cytokine responses and therefore are used as non-pathogenic arenavirus models in comparison with their closely related pathogenic counterparts, i.e.

LASV and JUNV, respectively (29, 30). This raises a question whether the highly conserved NP ExoN activity has additional function besides immune evasion. Furthermore, LASV ExoN- NP mutant protein demonstrated decreased capability to support LASV minigenome replication (31, 32), implying NP ExoN participates in LASV replication. Interestingly, positive-sense RNA virus coronavirus also possesses the same DEDDh ExoN motif in nsp14, which is essential for the fidelity of coronavirus RNA replication (33-35). Therefore, further studies are needed to investigate whether LASV NP ExoN motif has additional role in virus life cycle.

In present study, we rescued an ExoN-deficient LASV mutant (ExoN- rLASV) using reverse genetics system and found that loss of ExoN activity resulted in impaired virus growth and viral RNA replication in interferon-deficient cells. We also provide the evidence that abrogation of LASV NP ExoN increased aberrant viral RNA production in infection. Furthermore, ExoN-deficient LASV was more sensitive to mutagenic nucleoside analogue as compared with wild type LASV. Overall, our study indicates that LASV NP ExoN has previously unrecognized function in viral RNA replication besides its role in immune evasion. Our new finding may enhance our understanding of the basic virology of this important human pathogen.

Results

Abrogation of NP ExoN activity impaired LASV multiplication in interferon-deficient cells.

Biochemical studies have demonstrated that mutation of any of the NP D389, E391, D466, D533 and H528 residues diminished LASV NP ExoN activity. In LASV

minigenome replication system, NP D389A and D389AG392A mutants exhibited an impaired capability to support reporter gene expression (31, 32), suggesting NP ExoN activity is required for optimal LASV replication. To investigate the role of LASV ExoN in virus infection, we attempted to rescue recombinant LASV (rLASV, Josiah strain) harboring NP D389A and NP D389AG392A mutations by using murine Pol I promoter based LASV reverse genetics system. To minimize the likelihood of reverse mutation, two nucleotide substitution were introduced to mutate NP D380 and NP G392 residue. Specifically, for NP D380A mutant, nt $GA_{1266}C_{1267}$ in S agRNA was mutated to $GC_{1266}T_{1267}$. For NP D389AG392A mutant, $GA_{1266}C_{1267}$ (D389) and $GG_{1275}A_{1276}$ (G392) were mutated to $GC_{1266}T_{1267}$ (A389) and $GC_{1275}T_{1276}$ (A392), respectively. The rLASV NPD389A mutant (ExoN- rLASV hereafter) was successfully rescued. Sequencing analysis confirmed the introduced mutation is stable after 3 passages in Vero cells (Fig 2A). On the other hand, the rLASV NP D389AG392A mutant was not rescued despite repeated attempts, indicating rLASV with the NP D389AG392A mutation is not viable.

Next, we assessed the multiplication of ExoN- rLASV in interferon-deficient Vero cells (Fig 2B). Compared with wild-type (wt) rLASV, ExoN- rLASV demonstrated attenuated growth in Vero cells. At 48 hours post-infection (hpi), the virus titer of ExoN- rLASV was 51-fold and 835-fold lower at MOI 0.01 and MOI 1, respectively, than wt rLASV. Consistently, ExoN- rLASV also formed smaller plaques in Vero cells in comparison with wt rLASV (Fig 2C). Thus, abrogation of ExoN activity impaired rLASV propagation in Vero cells.

NP ExoN deficiency impaired LASV RNA replication in interferon-deficient cells.

As Vero cells are IFN-deficient (36, 37), the impaired multiplication of ExoN- rLASV in Vero cells attests to a role of NP ExoN in LASV replication other than IFN evasion. Given the role of coronavirus nsp14 DEDDh ExoN activity in coronavirus RNA replication, we reasoned that LASV NP ExoN is also involved in viral RNA replication.

Vero cells were infected with wt rLASV and ExoN- rLASV at MOI 0.01 for 72 hr or at MOI 1 for 24 hr. The virus titer of ExoN- rLASV was 51.4-fold and 6671-fold lower at MOI 0.01 and MOI 1, respectively, than wt rLASV, (Fig. 3A). To assess viral RNA level, total RNA was purified from infected cells and reverse transcribed to cDNA using random hexamer primers. Then, a qPCR assay was performed with NP specific primers to quantitate the viral RNA level at the NP locus, which measures the total RNA level of SgRNA, S agRNA and S mRNA (Fig 3B). Similarly, a qPCR assay with primers specific for the L locus was performed to measure the total RNA level of LgRNA, L agRNA and L mRNA (Fig 3C). At MOI 0.01, the ExoN- rLASV RNA level was 45.5-fold lower ($P<0.01$, student t test) at NP locus and 25.2-fold lower ($P=0.04$, student t test) at L locus than wt rLASV. At MOI 1, the ExoN- rLASV RNA level was 1637-fold lower ($P<0.01$, student t test) at NP locus and 122-fold lower ($P<0.01$) at L locus than wt rLASV.

We further examined the level of S gRNA and L gRNA. Reverse transcription (RT) was performed with primers targeting the 3'-end of S genomic RNA and L genomic RNA using high fidelity reverse transcriptase SuperScript IV (Invitrogen), followed by qPCR assays targeting NP locus on S gRNA and L locus on L gRNA as described above. At MOI 0.01, the level of ExoN- rLASV S gRNA and L gRNA were 62.3-fold lower ($P<0.01$, t test) and 16.7-fold lower ($P<0.02$), respectively, than wt rLASV. At MOI 1, the level of

ExoN- rLASV SgRNA and Lg RNA were 1181-fold (P<0.01, t test) lower and 387-fold (P<0.02) lower as compared with wt rLASV (Fig 3D and 3E). Overall, our data demonstrated that abrogation of ExoN led to substantially decreased LASV RNA production, to an extent largely comparable with virus titer reduction in IFN-deficient Vero cells.

Formation of aberrant viral RNA in ExoN- rLASV infection

Next, we performed RT-PCR to examine S gRNA and L gRNA in ExoN- rLASV infection. Vero cells were infected with wt rLASV and ExoN- rLASV at MOI 0.01 for 72 hrs or at MOI 1 for 24 hrs. Intracellular RNA samples were purified and reverse transcribed to cDNA using primers targeting the 3'-ends of S gRNA and L gRNA. Close-to-full-length S gRNA (3391 nt) and L gRNA (7265 nt) was amplified with high fidelity Platinum SuperFi DNA Polymerase (Invitrogen) to minimize PCR error. In agarose electrophoresis, we observed an aberrant S RNA product (indicated as S' in Fig 4A) migrating slightly faster than the standard S gRNA product (3391nt) in ExoN- rLASV samples both at MOI 0.01 and MOI 1. The aberrant S' product was detected specifically in ExoN- rLASV infection in repeated experiments. In L gRNA PCR, we also observed several aberrant L gRNA products (approximately 3.5 kb to 6 kb) in ExoN- rLASV samples both at MOI 0.01 and MOI 1 (Fig 4B). The result indicated that abrogation of NP ExoN activity increased aberrant Sg RNA and Lg RNA formation in LASV infection.

Abrogation of LASV NP ExoN activity affected the integrity of Sg RNA

To determine the sequence of the aberrant S' RNA in ExoN- rLASV infection, we performed agarose gel electrophoresis with ExoN- rLASV and wt rLASV PCR samples (MOI 1) and purified the PCR amplicons around the full-size of S segment. Purified

amplicons were cloned into cloning vector (pSMART, Lucigen). Sanger sequencing of 10 colonies identified two types of aberrant S RNAs formed in ExoN- rLASV infection. Three out of 10 colonies had a 37-nt deletion (S agRNA nt1824-1860), which is shown as the region from site I to site I' in Fig 5A and 5B. The 37-nt deletion is located in the 67-nt-long IGR and therefore could disrupt the stem-loop structure of IGR. In addition, five colonies contained a 231-nt deletion spanning the IGR and NP coding region (S agRNA nt1616-1846, from site II to II' in Fig 5C). The 231-nt deletion consists of 42 nts in IGR and 189 nts at the 3' end of NP gene (Fig 5C), which could disrupt IGR structure and cause reading frame shift from NP residue 507. In comparison, only 2 out of 10 colonies from wt rLASV S samples had the 37-nt deletion in IGR. These data indicated that LASV lacking NP ExoN activity is more prone to form structural deletion around S RNA IGR.

PacBio Single Molecule, Real-Time (SMRT) long-read sequencing to characterize aberrant S gRNA formed in ExoN- rLASV infection.

To systematically assess the spectrum of aberrant S gRNA formed in ExoN- rLASV infection, we utilize PacBio Single Molecule, Real-Time (SMRT) long-read sequencing technology (38) to characterize LASV SgRNA at single molecule level. In PacBio SMRT long-read sequencing, a DNA polymerase continues to read single circularized-cDNA-template for multiple rounds and provides deep sequencing data for each molecule. It can determine the circular consensus sequence (CCS) of full-length cDNA up to 10kb long at single molecule level with up to 99.99% accuracy. PacBio SMRT long-read sequencing is ideal for analyzing RNA quasi-species, long amplicons, and RNA structural variations. It has been successfully used in research works on RNA virus, for

example, studies on defective interference RNA in influenza virus infection and hepatitis C virus variants post drug treatment (39, 40).

We gel purified close-to-full-length S RNA PCR amplicon from wt- and ExoN- rLASV-infected cells (MOI 1) and performed PacBio SMRT long-read sequencing (Sequel II). A total of 402,410 CCS reads and 381,134 CCS reads was obtained for wt rLASV and ExoN- rLASV samples, respectively (Fig 6A). The mean number of read passes for each cDNA is 26 times for wt rLASV with an average length of 2319 nt and 28 times for ExoN- rLASV with an average length of 2319 nt (Fig 6A). The mean read score of the assay is >0.999. CCS reads with size of 3100-3391 bp were selected using Filter FASTQ and aligned with LASV reference sequence using *minimap2*. RNA variants with >3% frequency was called using *ivar*. In ExoN- rLASV sample, 88.9% and 4.9% of S RNA had the 231-nt and the 37-nt deletion (Fig 6B and 6C). In comparison, 7.1% and 18.2% of the S RNA had the 231-nt and the 37-nt deletion, respectively, in wt rLASV sample. The data also confirmed that greater than 99.93% of ExoN- rLASV harbored the intended NP D389A mutation. In addition, an A-to-G substitution at nt 393 (in antigenomic sense) was identified in S RNA in ExoN- rLASV sample at a frequency of 39.14%. A C-to-U substitution at nt 1518 in S RNA was found in wt rLASV sample with a frequency of 3.07%. Overall, the PacBio SMRT sequencing data confirmed that structural variations occurred at a substantially higher frequency in ExoN- rLASV S gRNA than wt rLASV S gRNA.

ExoN- rLASV was more sensitive to nucleoside analogue treatment.

Coronavirus nsp14 DEDDh 3’-5’ ExoN activity proofreads newly synthesized viral RNA by removing mis-incorporated nucleotide. Abrogation of nsp14 ExoN activity

rendered coronavirus susceptible to lethal mutagenesis when treated with nucleoside analogues such as 5-Fluorouracil (5-FU) (41). For prototype arenavirus LCMV, 5-FU also could be incorporated into nascent RNA in viral RNA synthesis and introduces mutations affecting LCMV fitness (42). It is possible that loss of ExoN activity could increase arenavirus sensitivity to mutagenic nucleoside analogues. Thus, we evaluated the sensitivity of wt rLASV and ExoN- rLASV to 5-FU in Vero cells (MOI 0.1). We first verified that 5-FU treatment alone did not affect cell viability at the concentrations administrated in the experiment (Fig. 7A, CellTiter-Glo Viability Assay, Promega). The result indicated that abrogation of NP ExoN activity substantially increased LASV sensitivity to 5-FU treatment starting from 100 µM (Fig 7B). At 400 µM, the ExoN-rLASV titer deceased by 1053-fold compared with the titer in mock-treated cells, which was 13.5-time greater than the 78-fold decrease for wt rLASV (Fig 7B).

EIDD-1931 (*N4*-hydroxycytidine or NHC) is a cytidine analogue that increases the mutation frequency of a broad range RNA viruses (43). We further assessed the sensitivity of ExoN- rLASV and wt rLASV to EIDD-1931. Treatment of Vero cells with EIDD-1931 (5 µM -100 µM) alone did not substantially affect cell viability (Fig 7A, CellTiter-Glo Viability Assay, Promega). At 100 µM EIDD-1931, the titer of ExoN- rLASV was decreased by 47.6-fold, greater than the 6-fold reduction for wt rLASV (Fig 7C). Collectively, our data indicated that abrogation of NP ExoN activity increased LASV sensitivity to mutagenic nucleoside analogues.

Discussion

LASV NP DEDDh motif has been known essential for LASV evasion of host innate immune and viral pathogenicity attributable to its ExoN activity to degrade dsRNA

generated in virus RNA replication. Interestingly, the DEDDh ExoN motif is highly conserved in arenavirus family, regardless of viral pathogenicity, implying the ExoN activity has yet-to-be-identified function(s) in arenavirus life cycle. Curiously, positive-sense RNA virus coronavirus contains the same DEDDh ExoN motif in nsp14, which has proofreading activity in viral RNA replication. In this study, we found that abrogation of NP ExoN attenuated LASV growth in IFN-deficient Vero cells. Furthermore, ExoN-rLASV demonstrated impaired viral RNA replication, including decreased S gRNA and L gRNA production, in IFN-deficient cells. For the first time, we found that ExoN- rLASV was prone to produce aberrant viral RNAs. Sanger sequencing and SMRT long-read sequencing of S RNA revealed that ExoN- rLASV is more likely to form structural deletions in S RNA, suggesting an impact of NP ExoN deficiency on viral genomic RNA integrity. In addition, we also found an increased sensitivity of ExoN- rLASV to mutagenic nucleoside analogue, suggesting NP ExoN has a role in reducing LASV RNA mutation. Taken together, our study provide evidence for previously unrecognized function(s) of LASV NP ExoN in optimal LASV RNA replication and control of aberrant viral RNA production and viral RNA mutation.

The data that NP ExoN deficiency affected the propagation and the plaque size of LASV in IFN-deficient Vero cells (Fig 2) clearly indicates an important role of NP ExoN in LASV fitness. This is also highlighted by our data that the NP D389AG392A rLASV mutant (Josiah strain) was not rescuable. Other studies have also documented that NP ExoN deficiency leads to attenuated growth of rPICV, rMOPV and rLASV (AV strain) in Vero cells (26, 27, 31). In addition, reversion to wt virus have been reported for ExoN-rPICV and ExoN- rLASV (AV strain) in IFN-deficient cells. PICV possessing NP D380A

mutation (equivalent to the NP D389A mutation for LASV) forms smaller plaques. After two passages of the PICV NP ExoN- mutant in Vero cell, wt revertant PICV, which forms large plaques, could be readily identified (27). For LASV AV strain, an NP D389A mutant was found partially reverted to wt sequence after two passages in Vero cells (31). Overall, ours and others' data indicated NP ExoN activity is required for optimal arenavirus replication.

There seems to be some differences in terms of the genetic stability of LASV NP ExoN- mutants in our study with the LASV Josiah strain and the study with LASV AV strain (31). For LASV AV strain, an NP D389AG392A mutant was rescued and genetically stable, while an NP D389A mutant partially reverted to wt sequence. In comparison, our data with the Josiah strain indicated the LASV NP D389AG392A mutant could not be rescued and the NP D389A mutation is stable at least after 3 passages in Vero cells. The reason for these discrepancies is unclear, probably due to virus strain difference. It is also possible that the two-nucleotide substitution in NP D389A mutant in present study reduced the likelihood of reversion to wt sequence. Nevertheless, both studies generally support for the involvement of NP ExoN in optimal LASV replication and fitness.

Our data further showed that abrogation of NP ExoN activity impaired LASV RNA replication, including S gRNA and L gRNA accumulation, in IFN-deficient cells (Fig 3). These findings are in line with previous studies, in which NP D389A mutant protein and NP D389AG392A mutant protein exhibited an impaired capability to support reporter gene expression in LASV minigenome replication systems (31, 32). Future studies are necessary to determine whether NP ExoN deficiency affects LASV genomic RNA

replication, mRNA transcription, or both. The RNA replication of RNA virus is error prone. Nucleotide mis-incorporation could cause viral RdRp stop or pause RNA elongation. As MOPV NP and LCMV NP are able to excise mismatched nucleotide at the 3'-end of dsRNA substrate (28), it is possible that NP ExoN is capable of removing mis-incorporated nucleotide in viral RNA synthesis and facilitating viral RNA synthesis. In this scenario, NP ExoN deficiency may affect the yield or the rate of viral RNA synthesis, which may partly explain the impaired viral RNA replication in ExoN- rLASV infection. Other than LASV, NP ExoN activity is also required for optimal reporter gene expression in PICV minigenome replication (27). Hence, it is interesting to study whether NP ExoN is required for optimal viral RNA replication for other arenaviruses.

An important finding of the present study is that abrogation of NP ExoN increased aberrant LASV RNA formation in LASV, which links NP ExoN activity to the integrity of viral genomic RNA. For the first time, we detected increased aberrant S gRNA and Lg RNA production in ExoN- rLASV-infected cells in repeated experiments (Fig 4). Sanger sequencing of close-to-full-length S gRNA amplicon revealed two type of deletion mutants in ExoN- rLASV samples. Three of 10 colonies had a 37-nt deletion (nt1824-1860, S agRNA) located in the 67-nt-long IGR (site I to site I' shown in Fig 5A and 5B). Five colonies contained a 231-nt deletion (nt1616-1846 in S agRNA, from II to II' shown in Fig 5C) in the IGR and NP coding region. The 37-nt deletion could disrupt the stem-loop structure in IGR. The 231-nt deletion could also disrupt IGR structure and cause reading frame shift from NP residue 507. In comparison, only 2 out of 10 colonies from wt rLASV S samples had the 37-nt deletion in IGR. The biological implication of these deletions remains to be investigated in further studies. Of note, arenavirus IGR is the

termination signal of viral mRNA transcription and also an viral RNA element for efficient viral genomic RNA packaging into progeny virus particles. Hence, abrogation of NP ExoN activity may indirectly affect proper viral mRNA synthesis as well as the efficacy of viral RNA packaging into virions.

To better understand the spectrum of LASV SgRNA variants, we further utilized PacBio SMRT long-read sequencing to characterize LASV SgRNA amplicon at single molecule level. Short-read Illumina NGS has low sensitivity or high false positive rates in solving complex Structural Variations (SVs) with deletions and insertions at least 50 nt in size (44). PacBio SMRT long-read sequencing can determine the circular consensus sequence of full-length cDNA up to 10kb long at single molecule level, which is ideal for analyzing RNA quasi-species, long amplicons, and SVs. In addition, SMRT long-read technology is ideal for sequencing through highly repetitive, GC-rich sequences that are presented in the IGR of arenavirus RNA. To ensure the accuracy of the SMRT assay, raw reads with a minimum number of passes greater than 3 and higher than 99% accuracy were used to generate the CCS reads. The mean number of read passes for each cDNA was 26 times for wt rLASV with an average length of 2319 nt and 28 times for ExoN- rLASV with an average length of 2319 nt (Fig 6A). The mean reading score of the SMRT assay was >99.9%. Variants of >3% frequency was selected in data analysis to ensure the reliability of the reads. The result indicated that 88.9% and 4.9% of the S genomic RNA contained the 231-nt deletion and the 37-nt deletion in ExoN- rLASV sample. In comparison, only 7.1% and 18.2% of the S RNA in wt rLASV sample has the 231-nt deletion and the 37-nt deletion. The data suggests NP ExoN helps to reduce structural deletion in viral genomic RNA. In addition, we found that

368 higher than 99.93% of ExoN- rLASV S gRNA harbored the intended NP D389A
369 mutation, which confirmed that the NP D389A mutation was maintained in ExoN-
370 rLASV.
371 The molecular basis for these structural deletions formed in ExoN- rLASV S RNA is
372 unclear. Interestingly, sequence analysis revealed the presence of homologous
373 sequences flanking the 37-nt deletion and the 231-nt deletion in S RNA (Fig 8, boxed
374 sequences, sites I/I' for the 37-nt deletion, sites II/II' for the 231-nt deletion).
375 Accordingly, we propose a stop-and-realign model for the mechanism of increased S
376 RNA structural deletions in ExoN- rLASV infection (Fig 8). MOPV NP ExoN and LCMV
377 NP ExoN excise mismatched nucleotide at the 3'-end of dsRNA substrate (28). When
378 viral RNA synthesis error occurs, LASV NP ExoN may also excise mismatched
379 nucleotide like MOPV and LCMV counterparts and facilitate RdRp L protein resume
380 RNA elongation. Without NP ExoN activity, viral RNA synthesis may stop as shown in
381 Fig 8A for the 37nt-deletion and Fig 8B for the 231nt-deletion (Step 1, mis-incorporation
382 and stop). Depending on the nucleotide mis-incorporated, LASV RdRp L protein may
383 realign the 3'-end of nascent RNA (at site I in Fig 8A and site II in Fig 8B) with
384 downstream homologous sequences on the template RNA (sites I' and II' in Fig 8A and
385 Fig 8B, respectively) and resume RNA elongation (Step 2, realign and resume)).
386 Consequently, the regions between these homologous sequences are skipped by RdRp
387 L protein, leading to the 37-nt deletion (Fig 8A) and the 231-nt deletion (Fig 8B) in S
388 RNA. Thus, LASV NP ExoN may act to reduce these structural deletions around IGR by
389 enhancing the fidelity of LASV RNA synthesis. In this regard, it is worth noting that RNA
390 viruses with low-fidelity RdRp, such as Sindbis virus or tombusvirus, exhibited an

increased production of defective viral genomic RNA correlated with an enhanced rate of viral RNA recombination (45-47). Further studies are warranted to investigate the molecular base of increased aberrant RNA formation associated with LASV NP ExoN deficiency.

Our nucleoside analogue data support for a role of LASV NP ExoN in reducing RNA mutation. The RNA replication of RNA virus is generally error prone, which increases the diversity of virus population that could be advantageous in evolution. However, the mutation rate should also be controlled as even a moderate 1.1-2.8-fold increase in mutation rate may drastically affect virus fitness (48). How arenavirus controls mutation is largely unknown. In LCMV infection, 5-FU could be incorporated into nascent viral RNA and cause mutations that severely affect LCMV fitness. We found that abrogation of NP ExoN activity increased LASV sensitivity to 5-FU as well as another mutagenic nucleoside analogue EIDD-1931 (Fig 7). These data suggest LASV NP ExoN activity contributes to reduce viral RNA mutation and enhance the fidelity of viral RNA replication.

In summary, the present study provided evidence that LASV NP ExoN is multifunctional, which is required for optimal viral RNA replication in addition to its recognized role in immune evasion. Abrogation of LASV NP ExoN activity leads to decreased viral RNA replication, increased aberrant viral RNA formation, and enhanced sensitivity to mutagenic nucleotide analogue. These findings provide novel and important insights into the role of NP ExoN motif in LASV life cycle. Future studies are warranted to investigate whether the NP ExoN of other arenaviruses also play roles in viral RNA replication. Hemorrhagic fever-causing arenaviruses continue to pose a threat

to public health with pandemic potential. A better understanding of the function of NP ExoN might inform vaccine and antiviral development against these important human pathogens.

Methods

Cells and Viruses.

Vero cells (CCL-81, ATCC) were maintained in Dulbecco's modified eagle medium (Hyclone) supplemented with 10% FBS (Invitrogen) and 1% penicillin and streptomycin solution (Hyclone). The LASV (Josiah strain) used in studies was recombinant virus that were rescued using reverse genetic systems in BHK21 cells and passaged only once (P1) in Vero cells as previously described (49). All plasmids used for LASV rescue were sequencing confirmed. Site-directed mutagenesis on p-mPol I-LASV Sag plasmid was performed using QuikChange II kit (Agilent) according to the instruction of manufacturer. To construct the rLASV NPD380A mutant, forward primer 5'-CCAAATGCTAAGACCTG GATGGCTATTGAAGGAAGACCTGAAGATC-OH, and reverse primer 5'-GATCTTCAG GTCTTCCTTCAATAGCCATCCAGGT CTTAGCATTTGG-OH were used. To construct the rLASV NP D389AG392A mutant, forward primer 5'-AAATGCTAAGACCTGGATGG CTATTGAAGCTAGACCTGAAGATCCAGTGG-OH, and reverse primer 5'-CCACTGGA TCTTCAGGTCTAGCTTCAATAGCCATCCAGGTCTTAGCATTT-OH were used. The sequence of mutant rLASV was confirmed by Sanger Sequencing after RT-PCR amplification of viral RNA extracted from infected cells. All infection work with pathogenic arenaviruses was performed at the BSL4 facilities in Galveston National Laboratory in the University of Texas Medical Branch in accordance with institutional health and safety guidelines and federal regulations.

RNA Extraction, RT-PCR and real-time RT-qPCR

RNA lysates were prepared using the TRIzol reagent (Life Technology). RNA was purified using the RNeasy Minikit (Qiagen) and treated with DNase I (Qiagen) as previously reported (32, 50). Equal amount of total RNA (0.5 to 1µg) was reverse transcribed to cDNA at 55 ^{o}C for 60 minutes using high fidelity reverse transcriptase SuperScript IV (Invitrogen) per manufacturer's protocol. The high-fidelity reverse transcriptase SuperScript IV has low RNase H activity and is suitable for long cDNA synthesis. Random hexamer primers and sequence specific primers were used in RT as specified in each experiment. cDNA samples were treated with RNase H. In RT of S gRNA, an S gRNA 3'UTR specific primer (5'-CGCACAGTGGATCCTAGGCTA-OH) was used. In RT of L gRNA, an L gRNA 3'UTR specific primer (5'- CACCGAGGATCCTAGG CATTAAGGCTATC-OH) was used in cDNA synthesis. PCR amplification of close to full-length Sg cDNA (3391bp) was conducted with Platinum SuperFi DNA Polymerase (Invitrogen) using forward primer 5'-ATCCTAGGCATTTTT GGTTGC-OH and reverse primer 5'-CGCACAGTGGATCCTAGGCTA-OH. PCR amplification of close to full-length Lg cDNA (7265 bp) was conducted with Platinum SuperFi DNA Polymerase using forward primer 5'-CACCGAGGATCCTAGG CATTAAGGCTATC-OH and reverse primer 5'-ATCCTAGGCAATTTGGTTGTTCTTTTTTGAG-OH. Real-time quantitative PCR (qPCR) was performed with SsoAdvanced Universal SYBR green Supermix (BioRad) on a CFX96 real-time PCR detection system (BioRad) as described previously (32, 50). To measure the viral RNA level at NP locus and L locus, cDNA synthesized with random primers was used in qPCR assay. LASV NP forward primer (5′-GAAGGGCCTG GGAAAACACT-OH) and LASV NP reverse primer (5′-AGGTAAGCCCAGCGGTAAAC-

OH) were used for NP locus. LASV L forward primer (5′-CAGCAGGTCAGACGAAGTG T-OH) and LASV L reverse primer (5′-GTTGTGCATAGGGGAGGCTT-OH) were used for L locus. To measure LASV Sg RNA and Lg RNA level with qPCR, cDNA synthesized with SgRNA- and LgRNA-specific primers as indicated above was used in qPCR assay. The qPCR data was analyzed with CFX Manager software (BioRad). The RNA level of each target gene was normalized to that of housekeeping gene β-actin with validated primers from BioRad. All experiments were performed separately in triplicates.

PacBio SMRT long-read sequencing of LASV SgRNA

Vero cells was infected by ExoN- rLASV and wt rLASV at MOI 1. At 48 hpi, total RNA was purified from infected cells. RT-PCR amplification of the close-to-full-length SgRNA was performed as described above. PCR amplicons (approximately 3.4 kb) were gel purified with Monarch DNA gel extraction kit (NEB). Library construction, PacBio SMRT long-read sequencing and CCS determination was performed by Azenta Life Sciences (USA). At least 1µg amplicon was ligated to barcoded adapters (Pacific Biosciences) for SMRTbell library construction and then sequenced on the PacBio Sequel IIe platform with v3.0 chemistry. Raw reads with a minimum number of passes greater than 3 were used to generate the CCS reads using PacBio SMRTLINK v.10.1. HiFi reads (>=99% accuracy) were extracted. Data analysis was performed utilizing *Galaxy*, an open source, web-based platform supported by NIH, NSF and the Texas Advanced Computing Center. CCS reads were filtered for those with size 3100-3394bp and high-quality reads (Phred>20) using Filter FASTQ and mapped to the LASV reference seq (MH358389) with *minimap2* (PacBio HiFi reads vs reference mapping (-k19 -w19 -

U50,500 -g10k -A1 -B4 -O6,26 -E2,1 -s200)). Variants with cutoff >3% frequency were called with *ivar* and visualized using the Integrated Genomics Viewer (IGV).

Mutagenic nucleotide analogue treatment

5'-fluorouracil (Cat# 03738, Sigma) and N4-hydroxycytidine (EIDD-1931) (Cat#9002958, Cayman) were dissolved in DMSO (cell culture grade, Sigma) and further diluted in DMEM media contain 2% FBS and 0.1% DMSO. Vero cells were mock-treated or treated with 5-FU or EIDD-1931 at different concentrations as indicated in each experiment for 4 hrs and then infected with wt rLASV and ExoN- rLASV (MOI 0.1) for 1 hr. Virus inoculums were removed and replaced with fresh media (DMEM + 2% FBS and 0.1% DMSO) containing 5-FU or EIDD-1931 of different concentrations as indicated. At 48 hpi, the supernatants of infected cells were harvested and subjected to plaque assay to determine virus titers. The viability of Vero cells treated with 5-FU and EIDD-1931 alone were assessed using CellTiter-Glo Viability Assay (Promega).

Acknowledgments

This work was supported in part by Public Health Service grants 1R21AI166985 (to CH) RO1AI093445 (to SP) and RO1AI129198 (to SP). CH was also supported by Institute for Human Infections & Immunity, UTMB Pilot Study Fund (P86035) and would like to acknowledge Galveston National Laboratory (supported by the Public Health Service award 5UC7AI094660) for support of research activity. Research work in Dr. Paessler's lab was also supported by the John. S. Dunn Distinguished Chair in Biodefense endowment. E.K.M was supported by National Institutes of Health T32 training grant AI060549.

Figure legends

Figure 1. (A). Schematic diagram of arenavirus S and L genomic RNAs. On each genomic RNA, an Intergenic Region (IGR) separates two ORFs. The highly structured IGRs are the termination signals of viral mRNA transcription and required for efficient packaging of viral genomic RNA into progeny viruses. **(B).** Genomic RNA replication and mRNA transcription of arenavirus S RNA. After virus entry, L protein and NP transcribe NP mRNA from S gRNA. S antigenomic RNA (S agRNA) is also synthesized from S gRNA, which serves as the template for GPC mRNA and S gRNA synthesis later in virus infection. Arenavirus mRNA lacks a poly-A tail and contains the structured IGR at 3'-end.

Figure 2. Abrogation of NP ExoN activity impaired LASV multiplication in interferon-deficient cells.

A recombinant LASV (rLASV) with NP D389A mutation was rescued (ExoN- rLASV). (A). The D389A mutation was maintained after 3 passages in Vero cells (Sanger sequencing). (B). The growth curve of wild-type rLASV (wt) and the ExoN- rLASV (NP ExoN-) in Vero cells at multiplicity of infection (MOI) 0.01 and MOI 1. (C) The plaque morphology of wt rLASV (wt) and ExoN- rLASV.

Figure 3. Abrogation of NP ExoN activity affected LASV RNA replication.

Vero cells were infected with wt rLASV and ExoN- rLASV (MOI=0.01 and 1.0). At 72 hpi (MOI 0.01) or 24 hpi (MOI 1.0), virus titer was determined by plaque assay **(A)**. RT-

qPCR assay for viral RNA level at the NP locus **(B)** and L locus **(C)**. The viral RNA level for S gRNA **(D)** and L gRNA **(E)** were also determined by qRT-PCR. The viral RNA level was normalized to the level of host β-actin mRNA and are presented as the fold changes relative to the level of ExoN- rLASV samples (set as 1.0). The data presents the mean and SEM of three independent experiments. (*: P<0.01; **: P<0.02; ***: P<0.05 with Student *t*-test).

Figure 4. Aberrant viral RNA formation in ExoN- rLASV infection

Vero cells were infected with wt rLASV (wt) and ExoN- rLASV (ExoN-) at MOI 0.01 for 72 hr and at MOI 1 for 24 hr. RNA samples were purified from infected cells and transcribed to cDNA with primers targeting the 3'-end of S gRNA and L gRNA, respectively. High-fidelity PCR was performed to amplify close-to-full-length S gRNA (3391 nt) and L gRNA (7265 nt) followed by agarose gel electrophoresis. (**A**). RT-PCR result of S gRNA (S). S' is a slightly fast-migrating aberrant S RNA product in ExoN- rLASV samples. (**B**). RT- PCR result of L gRNA. Several aberrant L gRNA products in ExoN- rLASV samples (3.5 kb to 6 kb) are observed. The aberrant RNA products are indicated by asterisk (*). Plasmid: PCR product using a plasmid containing LASV L segment as template.

Figure 5. Sanger sequencing of aberrant S RNA formed in ExoN- rLASV infection.

(A). Predicted RNA structure of IGR of S RNA by *mFold.* **(B).** In ExoN- rLASV, a 37-nt deletion (nt1824-1860 in S agRNA) from site I to site I' disrupted IGR structure. **(C)** a 231-nt deletion (nt1616-1846 in S agRNA) from C-terminus of NP at site II' to site II in IGR (refer to A) was identified in S gRNA sample of ExoN- rLASV.

Figure 6. PacBio SMRT long-read sequencing of S gRNA in rLASV samples.

Vero cells were infected with wt rLASV and ExoN- rLASV (MOI 1.0). RT-PCR product of the close-to-full-length SgRNA (3391 nt) were purified after agarose gel electrophoresis and subjected to PacBio SMRT long-read sequencing (Sequel IIe) with v3.0 chemistry. **(A).** HiFi CCS reads were generated using PacBio SMRTLINK v.10.1. **(B).** CCS reads with size 3100-3391bp were selected with Filter FASTQ and mapped to LASV reference seq (GenBank MH358389) with *minimap2.* Variants were called with *ivar* and visualized using the Integrated Genomics Viewer. **(C)**. The percentage of the 231-nt deletion and the 37-nt deletion in S RNA of wt rLASV and ExoN- rLASV sample.

Figure 7. NP ExoN deficiency enhanced LASV sensitivity to mutagenic nucleotide analogues.

(A). Vero cells were treated with 5'-FU and EIDD-1931 at indicated concentrations. At 48 hr post treatment, cell viability was measured using CellTiter-Glo Viability Assay (Promega). Data shown are the average (n=4) and SEM. **(B) and (C).** Vero cells were treated with 5-FU and EIDD-1931 at different concentrations as indicated. Cells were infected with wt rLASV (wt) and ExoN- rLASV (ExoN-) at MOI 0.1. At 48 hpi, virus titers were determined by plaque assay. Log10 virus titer changes relative to the virus titer of non-treated cells are shown. Data presented are the mean and the SEM of three independent experiments.

Figure 8. A stop-and-realign model for the 37-nt deletion **(A)** and the 231-nt deletion **(B)** in S RNA of ExoN- rLASV. Homologous sequences flanking the deletion sites are indicated as boxed sequences (sites I/I' for the 37-nt deletion, sites II/II' for the 231-nt deletion). Sites I and II are located in IGR stem-loop structure. In viral RNA synthesis, NP ExoN may remove the mis-incorporated nucleotide and helps LASV RdRp L protein

to resume viral RNA elongation. In the absence of NP ExoN activity, viral RNA elongation may terminate (Step 1). Depending on the nucleotide mis-incorporated (i.e., an A instead of C as shown in A and B), viral RdRp L protein may realign the 3'-end of nascent RNA (site I or II) with downstream homologous sequences on the template RNA (Sites I' and II') and resume RNA elongation (Step 2). Thus, the 37-nt deletion and the 237-nt deletion in S RNA may be derived from viral RdRp skipping the regions between the homologous sequences, an error could be controlled by functional NP ExoN.

References

1. Maes P, Adkins S, Alkhovsky SV, Avsic-Zupanc T, Ballinger MJ, Bente DA, Beer M, Bergeron E, Blair CD, Briese T, Buchmeier MJ, Burt FJ, Calisher CH, Charrel RN, Choi IR, Clegg JCS, de la Torre JC, de Lamballerie X, DeRisi JL, Digiaro M, Drebot M, Ebihara H, Elbeaino T, Ergunay K, Fulhorst CF, Garrison AR, Gao GF, Gonzalez JJ, Groschup MH, Gunther S, Haenni AL, Hall RA, Hewson R, Hughes HR, Jain RK, Jonson MG, Junglen S, Klempa B, Klingstrom J, Kormelink R, Lambert AJ, Langevin SA, Lukashevich IS, Marklewitz M, Martelli GP, Mielke-Ehret N, Mirazimi A, Muhlbach HP, Naidu R, Nunes MRT, et al. 2019. Taxonomy of the order Bunyavirales: second update 2018. Arch Virol 164:927-941.
2. Shi M, Lin XD, Chen X, Tian JH, Chen LJ, Li K, Wang W, Eden JS, Shen JJ, Liu L, Holmes EC, Zhang YZ. 2018. The evolutionary history of vertebrate RNA viruses. Nature 556:197-202.
3. Geisbert TW, Jahrling PB. 2004. Exotic emerging viral diseases: progress and challenges. Nat Med 10:S110-121.

4. Grant A, Seregin A, Huang C, Kolokoltsova O, Brasier A, Peters C, Paessler S. 2012. Junin virus pathogenesis and virus replication. Viruses 4:2317-2339.

5. Gunther S, Lenz O. 2004. Lassa Virus, vol 41, p 339-390, Critical Reviews in Clinical Laboratory Science.

6. Lukashevich IS. 2012. Advanced vaccine candidates for Lassa fever. Viruses 4:2514-2557.

7. McCormick JB, Webb PA, Krebs JW, Johnson KM, Smith ES. 1987. A prospective study of the epidemiology and ecology of Lassa fever. J Infect Dis 155:437-444.

8. Dan-Nwafor CC, Furuse Y, Ilori EA, Ipadeola O, Akabike KO, Ahumibe A, Ukponu W, Bakare L, Okwor TJ, Joseph G, Mba NG, Akano A, Olayinka AT, Okoli I, Okea RA, Makava F, Ugbogulu N, Oladele S, Namara G, Muwanguzi EN, Naidoo D, Mutbam SK, Okudo I, Woldetsadik SF, Lasuba CL, Ihekweazu C. 2019. Measures to control protracted large Lassa fever outbreak in Nigeria, 1 January to 28 April 2019. Euro Surveill 24.

9. Sattler RA, Paessler S, Ly H, Huang C. 2020. Animal Models of Lassa Fever. Pathogens 9.

10. Mateer EJ, Huang C, Shehu NY, Paessler S. 2018. Lassa fever-induced sensorineural hearing loss: A neglected public health and social burden. PLoS Negl Trop Dis 12:e0006187.

11. Gomez RM, Jaquenod de Giusti C, Sanchez Vallduvi MM, Frik J, Ferrer MF, Schattner M. 2011. Junin virus. A XXI century update. Microbes Infect 13:303-311.

12. Patterson M, Grant A, Paessler S. 2014. Epidemiology and pathogenesis of Bolivian hemorrhagic fever. Curr Opin Virol 5:82-90.

13. World Health Organization WH. 2018. 2018 Annual review of diseases prioritized under the Research and Development Blueprint. http://www.who.int/blueprint/priority-diseases/en/

14. Buchmeier MJ, de la Torre JC, Peters CJ. 2007. Arenaviridae: the viruses and their replication, 5th ed, vol 2. Wolter Kluwer Lippincott Williams & Wilkins, Philadelphia, PA, USA.

15. Pinschewer DD, Perez M, de la Torre JC. 2003. Role of the virus nucleoprotein in the regulation of lymphocytic choriomeningitis virus transcription and RNA replication. J Virol 77:3882-3887.

16. Baird NL, York J, Nunberg JH. 2012. Arenavirus infection induces discrete cytosolic structures for RNA replication. J Virol 86:11301-11310.

17. Dickson AM, Wilusz J. 2011. Strategies for viral RNA stability: live long and prosper. Trends Genet 27:286-293.

18. Ross J. 1995. mRNA stability in mammalian cells. Microbiol Rev 59:423-450.

19. Pinschewer DD, Perez M, de la Torre JC. 2005. Dual role of the lymphocytic choriomeningitis virus intergenic region in transcription termination and virus propagation. J Virol 79:4519-4526.

20. Hastie KM, Liu T, Li S, King LB, Ngo N, Zandonatti MA, Woods VL, Jr., de la Torre JC, Saphire EO. 2011. Crystal structure of the Lassa virus nucleoprotein-RNA complex reveals a gating mechanism for RNA binding. Proc Natl Acad Sci U S A 108:19365-19370.

21. Hastie KM, Kimberlin CR, Zandonatti MA, MacRae IJ, Saphire EO. 2011. Structure of the Lassa virus nucleoprotein reveals a dsRNA-specific 3' to 5' exonuclease activity essential for immune suppression. Proc Natl Acad Sci U S A 108:2396-2401.

22. Jiang X, Huang Q, Wang W, Dong H, Ly H, Liang Y, Dong C. 2013. Structures of arenaviral nucleoproteins with triphosphate dsRNA reveal a unique mechanism of immune suppression. J Biol Chem 288:16949-16959.

23. Qi X, Lan S, Wang W, Schelde LM, Dong H, Wallat GD, Ly H, Liang Y, Dong C. 2010. Cap binding and immune evasion revealed by Lassa nucleoprotein structure. Nature 468:779-783.

24. Mantlo E, Paessler S, Huang C. 2019. Differential Immune Responses to Hemorrhagic Fever-Causing Arenaviruses. Vaccines (Basel) 7.

25. Meyer B, Ly H. 2016. Inhibition of Innate Immune Responses Is Key to Pathogenesis by Arenaviruses. J Virol 90:3810-3818.

26. Carnec X, Mateo M, Page A, Reynard S, Hortion J, Picard C, Yekwa E, Barrot L, Barron S, Vallve A, Raoul H, Carbonnelle C, Ferron F, Baize S. 2018. A Vaccine Platform against Arenaviruses Based on a Recombinant Hyperattenuated Mopeia Virus Expressing Heterologous Glycoproteins. J Virol 92:J Virol 92:e0223017. https://doi.org/10.1128/JVI.0202230-0223017.

27. Huang Q, Shao J, Lan S, Zhou Y, Xing J, Dong C, Liang Y, Ly H. 2015. In vitro and in vivo characterizations of pichinde viral nucleoprotein exoribonuclease functions. J Virol 89:6595-6607.

28. Yekwa E, Aphibanthammakit C, Carnec X, Coutard B, Picard C, Canard B, Baize S, Ferron F. 2019. Arenaviridae exoribonuclease presents genomic RNA edition capacity. bioRxiv doi:10.1101/541698:541698.

29. Groseth A, Hoenen T, Weber M, Wolff S, Herwig A, Kaufmann A, Becker S. 2011. Tacaribe virus but not junin virus infection induces cytokine release from primary human monocytes and macrophages. PLoS Negl Trop Dis 5:e1137.

30. Pannetier D, Faure C, Georges-Courbot MC, Deubel V, Baize S. 2004. Human macrophages, but not dendritic cells, are activated and produce alpha/beta interferons in response to Mopeia virus infection. J Virol 78:10516-10524.

31. Carnec X, Baize S, Reynard S, Diancourt L, Caro V, Tordo N, Bouloy M. 2011. Lassa virus nucleoprotein mutants generated by reverse genetics induce a robust type I interferon response in human dendritic cells and macrophages. J Virol 85:12093-12097.

32. Mateer EJ, Maruyama J, Card GE, Paessler S, Huang C. 2020. Lassa Virus, but Not Highly Pathogenic New World Arenaviruses, Restricts Immunostimulatory Double-Stranded RNA Accumulation during Infection. J Virol 94:e02006-02019. https://doi.org/10.1128/JVI.02006-02019.

33. Denison MR, Graham RL, Donaldson EF, Eckerle LD, Baric RS. 2011. Coronaviruses: an RNA proofreading machine regulates replication fidelity and diversity. RNA Biol 8:270-279.

34. Minskaia E, Hertzig T, Gorbalenya AE, Campanacci V, Cambillau C, Canard B, Ziebuhr J. 2006. Discovery of an RNA virus 3'->5' exoribonuclease that is

critically involved in coronavirus RNA synthesis. Proc Natl Acad Sci U S A 103:5108-5113.

35. Ogando NS, Ferron F, Decroly E, Canard B, Posthuma CC, Snijder EJ. 2019. The Curious Case of the Nidovirus Exoribonuclease: Its Role in RNA Synthesis and Replication Fidelity. Front Microbiol 10:1813.

36. Osada N, Kohara A, Yamaji T, Hirayama N, Kasai F, Sekizuka T, Kuroda M, Hanada K. 2014. The genome landscape of the african green monkey kidney-derived vero cell line. DNA Res 21:673-683.

37. Desmyter J, Melnick JL, Rawls WE. 1968. Defectiveness of interferon production and of rubella virus interference in a line of African green monkey kidney cells (Vero). J Virol 2:955-961.

38. Rhoads A, Au KF. 2015. PacBio Sequencing and Its Applications. Genomics Proteomics Bioinformatics 13:278-289.

39. Lui WY, Yuen CK, Li C, Wong WM, Lui PY, Lin CH, Chan KH, Zhao H, Chen H, To KKW, Zhang AJX, Yuen KY, Kok KH. 2019. SMRT sequencing revealed the diversity and characteristics of defective interfering RNAs in influenza A (H7N9) virus infection. Emerg Microbes Infect 8:662-674.

40. Yamashita T, Takeda H, Takai A, Arasawa S, Nakamura F, Mashimo Y, Hozan M, Ohtsuru S, Seno H, Ueda Y, Sekine A. 2020. Single-molecular real-time deep sequencing reveals the dynamics of multi-drug resistant haplotypes and structural variations in the hepatitis C virus genome. Sci Rep 10:2651.

41. Smith EC, Blanc H, Surdel MC, Vignuzzi M, Denison MR. 2013. Coronaviruses lacking exoribonuclease activity are susceptible to lethal mutagenesis: evidence for proofreading and potential therapeutics. PLoS Pathog 9:e1003565.

42. Ruiz-Jarabo CM, Ly C, Domingo E, de la Torre JC. 2003. Lethal mutagenesis of the prototypic arenavirus lymphocytic choriomeningitis virus (LCMV). Virology 308:37-47.

43. Agostini ML, Pruijssers AJ, Chappell JD, Gribble J, Lu X, Andres EL, Bluemling GR, Lockwood MA, Sheahan TP, Sims AC, Natchus MG, Saindane M, Kolykhalov AA, Painter GR, Baric RS, Denison MR. 2019. Small-Molecule Antiviral beta-d-N(4)-Hydroxycytidine Inhibits a Proofreading-Intact Coronavirus with a High Genetic Barrier to Resistance. J Virol 93:e01348-01319. https://doi.org/10.1128/JVI.01348-01319.

44. Sedlazeck FJ, Rescheneder P, Smolka M, Fang H, Nattestad M, von Haeseler A, Schatz MC. 2018. Accurate detection of complex structural variations using single-molecule sequencing. Nat Methods 15:461-468.

45. Panaviene Z, Nagy PD. 2003. Mutations in the RNA-binding domains of tombusvirus replicase proteins affect RNA recombination in vivo. Virology 317:359-372.

46. Poirier EZ, Mounce BC, Rozen-Gagnon K, Hooikaas PJ, Stapleford KA, Moratorio G, Vignuzzi M. 2015. Low-Fidelity Polymerases of Alphaviruses Recombine at Higher Rates To Overproduce Defective Interfering Particles. J Virol 90:2446-2454.

47. Vignuzzi M, Lopez CB. 2019. Defective viral genomes are key drivers of the virus-host interaction. Nat Microbiol 4:1075-1087.

48. Holland JJ, Domingo E, de la Torre JC, Steinhauer DA. 1990. Mutation frequencies at defined single codon sites in vesicular stomatitis virus and poliovirus can be increased only slightly by chemical mutagenesis. J Virol 64:3960-3962.

49. Yun NE, Seregin AV, Walker DH, Popov VL, Walker AG, Smith JN, Miller M, de la Torre JC, Smith JK, Borisevich V, Fair JN, Wauquier N, Grant DS, Bockarie B, Bente D, Paessler S. 2013. Mice lacking functional STAT1 are highly susceptible to lethal infection with Lassa virus. J Virol 87:10908-10911.

50. Huang C, Kolokoltsova OA, Mateer EJ, Koma T, Paessler S. 2017. Highly Pathogenic New World Arenavirus Infection Activates the Pattern Recognition Receptor Protein Kinase R without Attenuating Virus Replication in Human Cells. J Virol 91:e01090-01017. https://doi.org/10.1128/JVI.01090-01017.

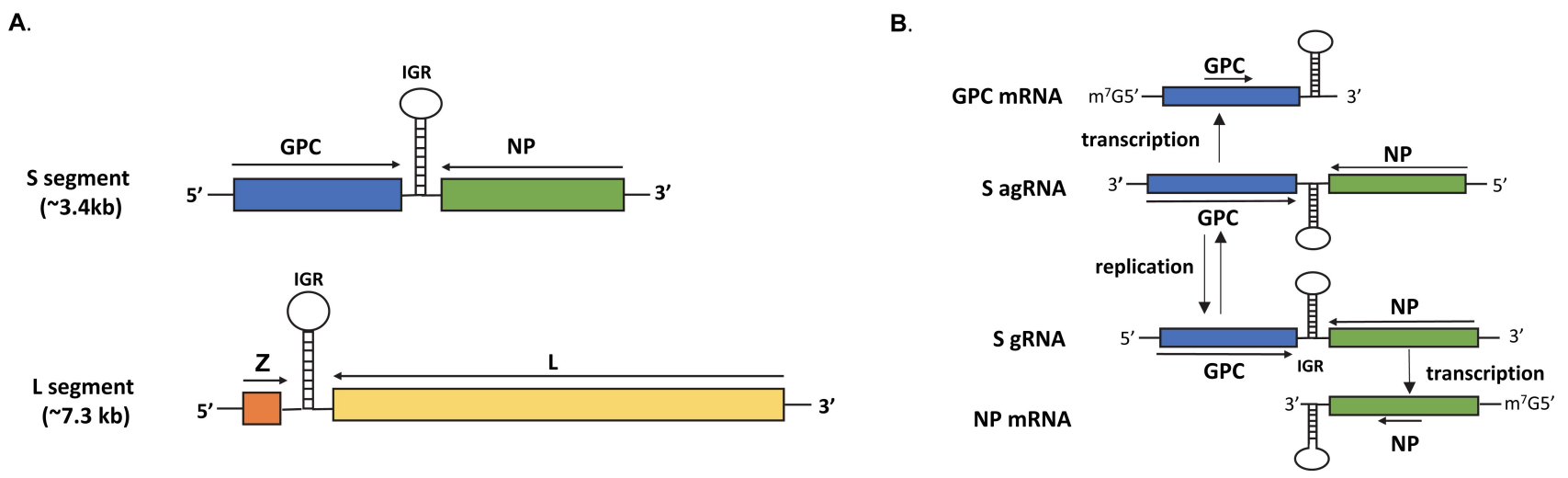
A.
IGR
GPC
NP
S segment
(~3.4kb)
5'
3'
IGR
Z
L
L segment
(~7.3 kb)
5'
3'
B.
GPC
GPC mRNA
m7G5'
3'
transcription
NP
S agRNA
3'
5'
GPC
replication
NP
S gRNA
5'
3'
GPC
IGR
transcription
NP mRNA
3'
m7G5'
NP

A.

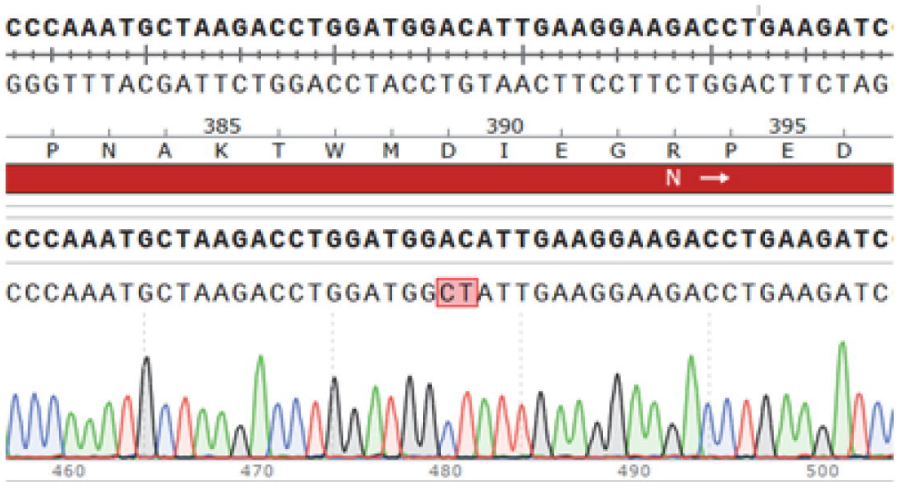
CCCAAATGCTAAGACCTGGATGGACATTGAAGGAAGACCTGAAGATC
GGGTTTACGATTCTGGACCTACCTGTAACTTCCTTCTGGACTTCTAG
385
390
395
P N A K T W M D I E G R P E D
N
CCCAAATGCTAAGACCTGGATGGACATTGAAGGAAGACCTGAAGATC
CCCAAATGCTAAGACCTGGATGGCTATTGAAGGAAGACCTGAAGATC
460
470
480
490
500

C.

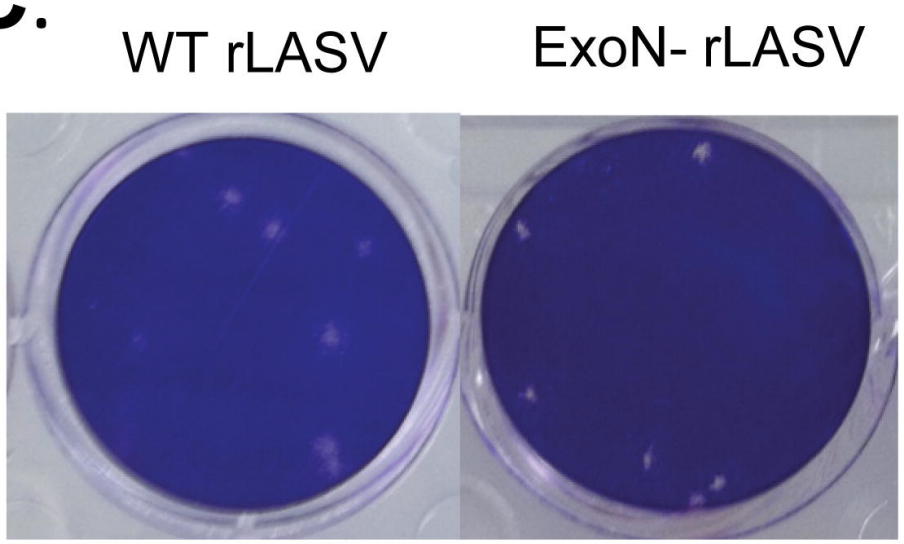
WT rLASV
ExoN- rLASV

B.

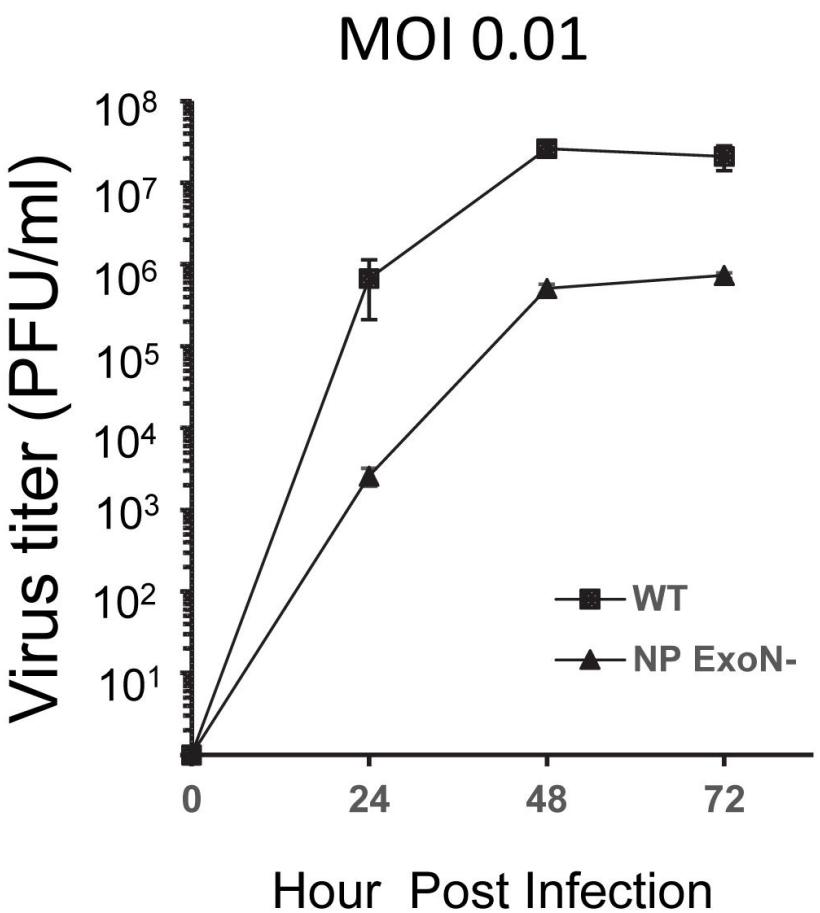
MOI 0.01
Virus titer (PFU/ml)
10^8
10^7
10^6
10^5
10^4
10^3
10^2
10^1
WT
NP ExoN-
0
24
48
72
Hour Post Infection

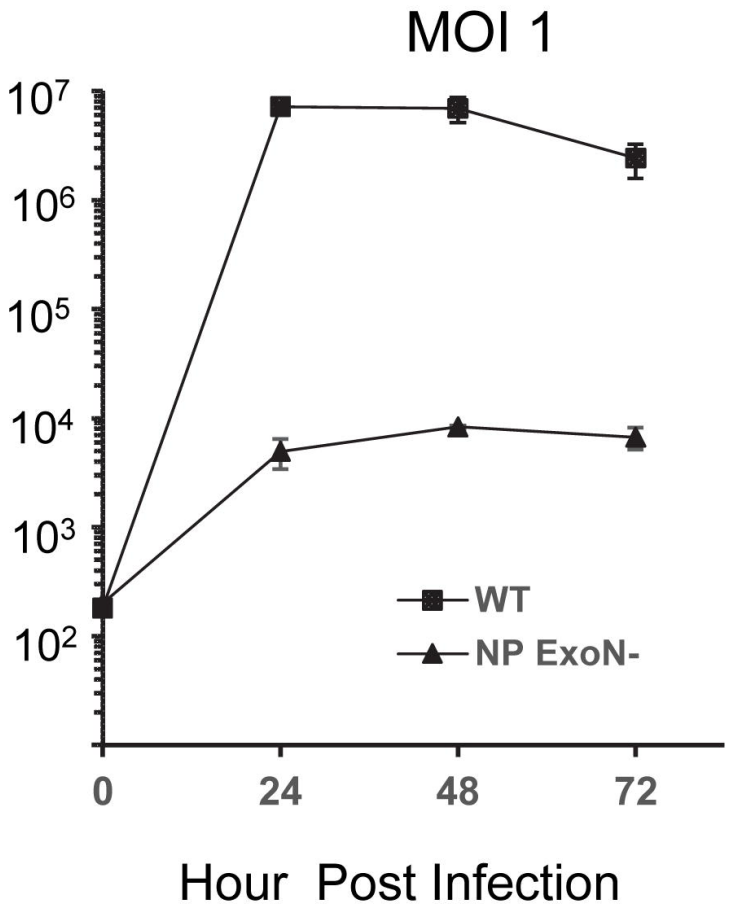
MOI 1
10^7
10^6
10^5
10^4
10^3
10^2
WT
NP ExoN-
0
24
48
72
Hour Post Infection

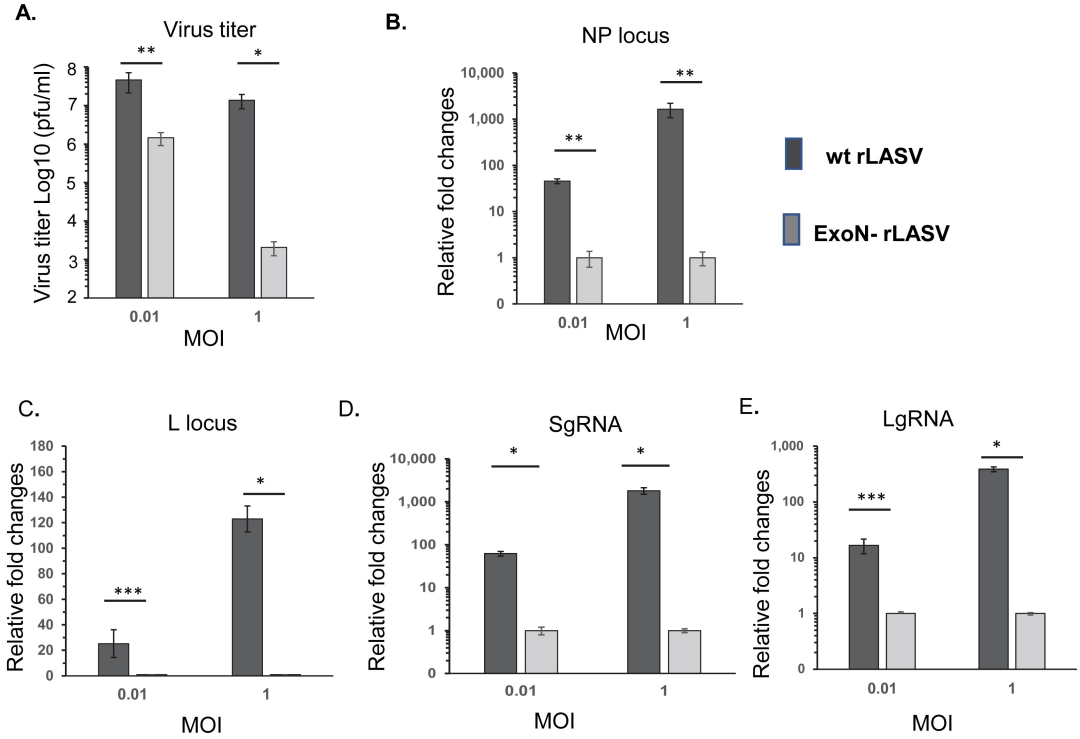
A.
Virus titer
Virus titer Log10 (pfu/ml)
8
7
6
5
4
3
2
**
*
0.01
1
MOI
B.
NP locus
Relative fold changes
10,000
1,000
100
10
1
0
**
**
0.01
1
MOI
wt rLASV
ExoN- rLASV
C.
L locus
Relative fold changes
180
160
140
120
100
80
60
40
20
0
***
*
0.01
1
MOI
D.
SgRNA
Relative fold changes
10,000
1,000
100
10
1
0
*
*
0.01
1
MOI
E.
LgRNA
Relative fold changes
1,000
100
10
1
0
***
*
0.01
1
MOI

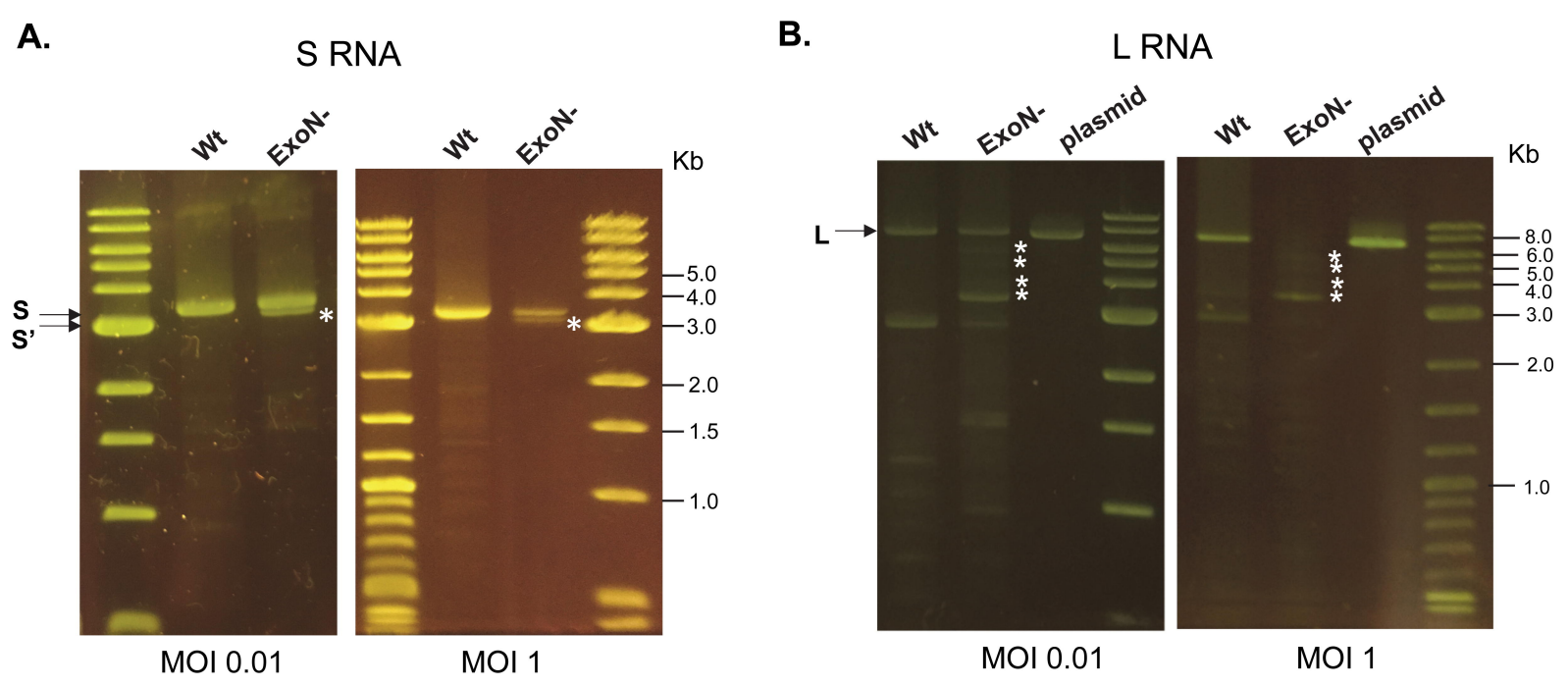
A.
S RNA
Wt
ExoN-
Wt
ExoN-
Kb
S
S'
*
*
5.0
4.0
3.0
2.0
1.5
1.0
MOI 0.01
MOI 1
B.
L RNA
Wt
ExoN-
plasmid
Wt
ExoN-
plasmid
Kb
L
***
***
8.0
6.0
5.0
4.0
3.0
2.0
1.0
MOI 0.01
MOI 1

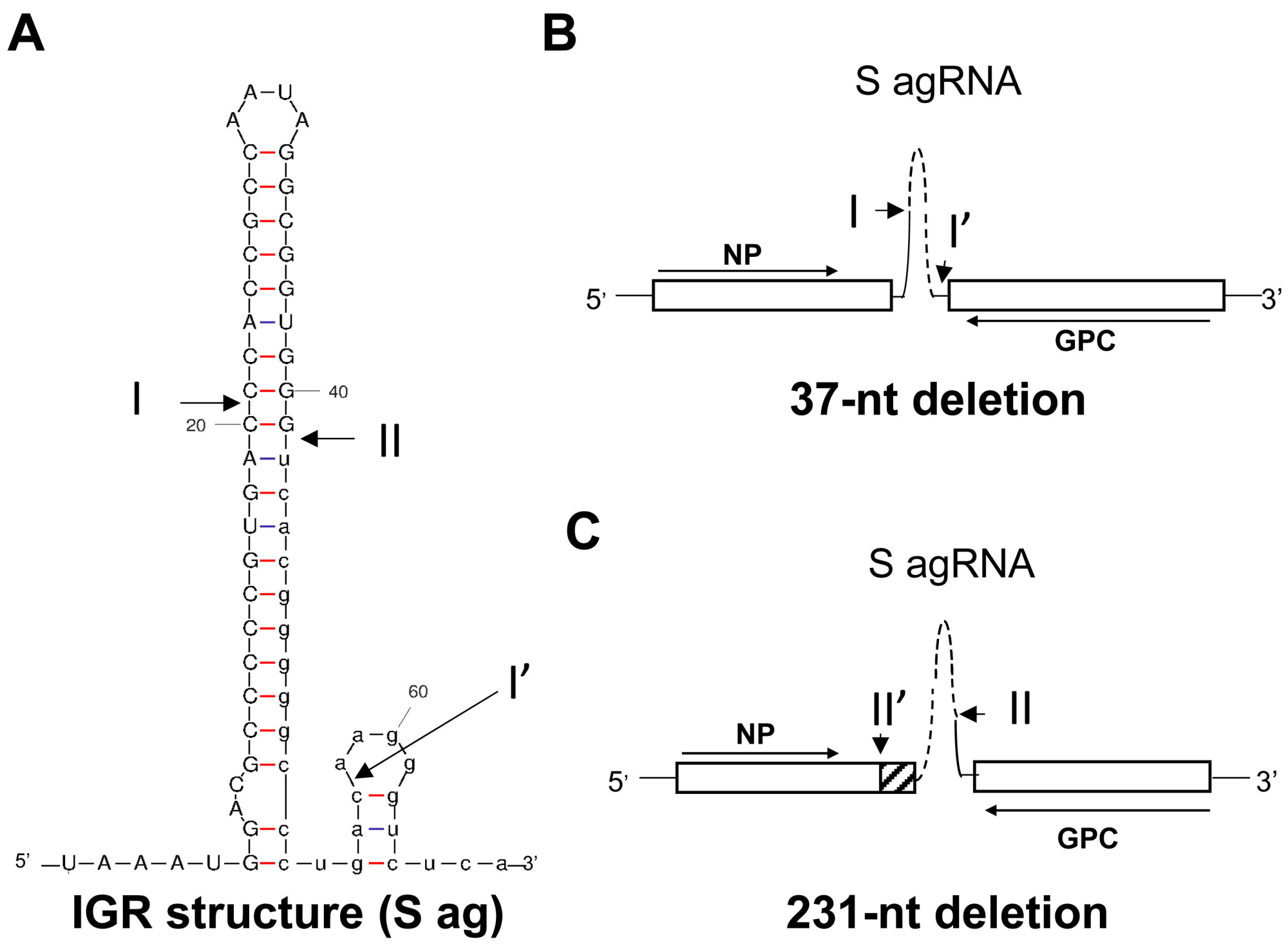
A
I
II
I'
20
40
60
5' —U—A—A—A—U—G—c—u—g—c—u—c—a—3'
IGR structure (S ag)
B
S agRNA
I
I'
NP
5'
3'
GPC
37-nt deletion
C
S agRNA
II'
II
NP
5'
3'
GPC
231-nt deletion

A.

Sample ID	CCS Reads	Number of CCS Bases	CCS Read Score (mean)	Number of Passes (mean)
Wt rLASV	402,410	933,554,242	0.999	28
ExoN- rLASV	381,134	994,863,239	0.999	26

B.

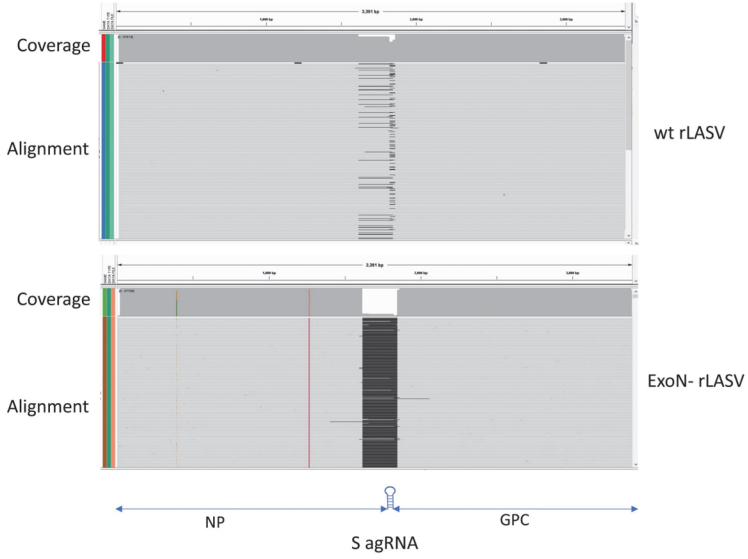

C.

Sample	231-nt del	37-nt del
Wt rLASV	7.1%	18.2%
ExoN- rLASV	88.9%	4.9%

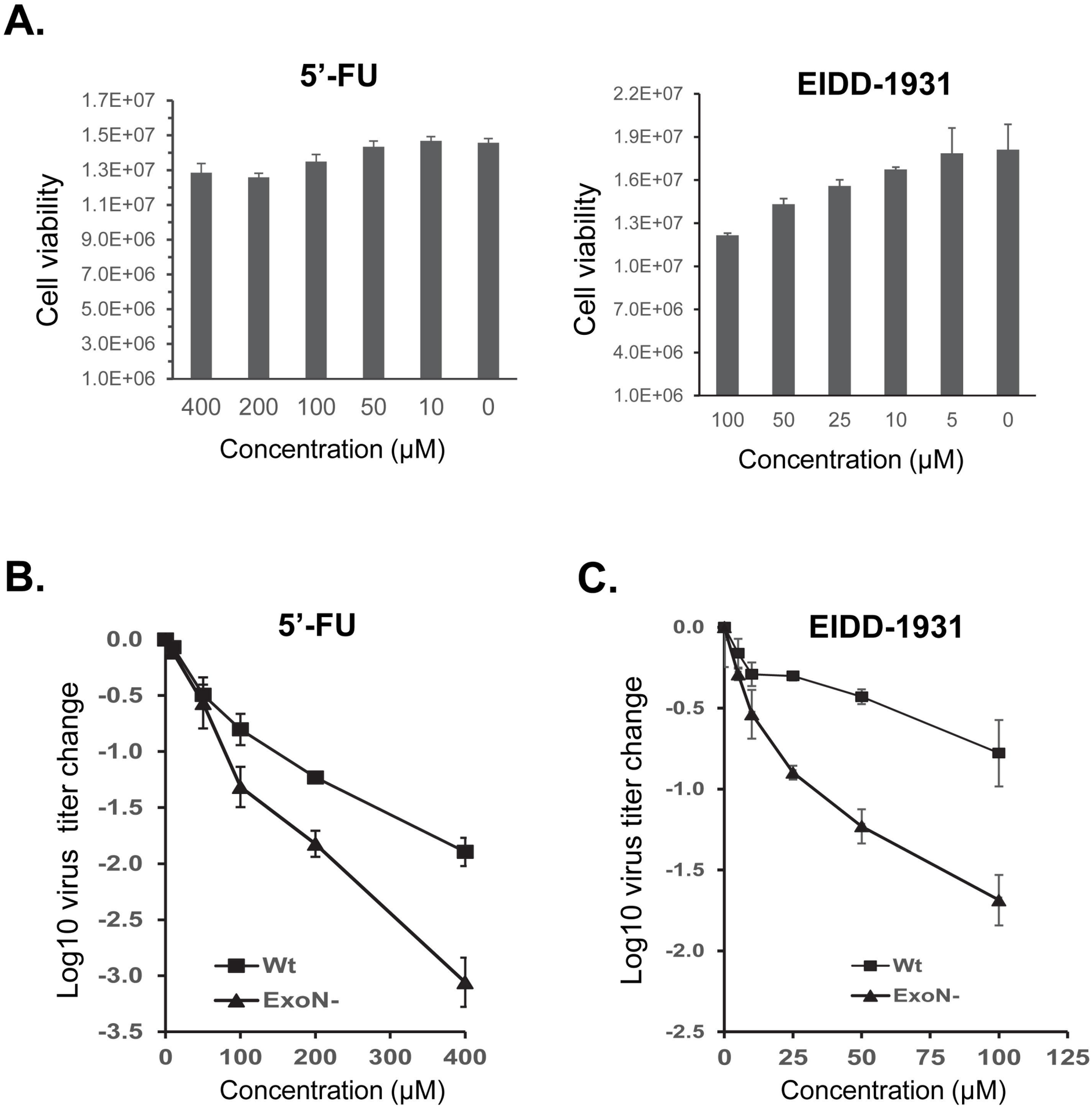
A.
5'-FU
Cell viability
1.7E+07
1.5E+07
1.3E+07
1.1E+07
9.0E+06
7.0E+06
5.0E+06
3.0E+06
1.0E+06
400 200 100 50 10 0
Concentration (μM)
EIDD-1931
Cell viability
2.2E+07
1.9E+07
1.6E+07
1.3E+07
1.0E+07
7.0E+06
4.0E+06
1.0E+06
100 50 25 10 5 0
Concentration (μM)
B.
5'-FU
Log10 virus titer change
0.0
-0.5
-1.0
-1.5
-2.0
-2.5
-3.0
-3.5
0 100 200 300 400
Concentration (μM)
Wt
ExoN-
C.
EIDD-1931
Log10 virus titer change
0.0
-0.5
-1.0
-1.5
-2.0
-2.5
0 25 50 75 100 125
Concentration (μM)
Wt
ExoN-

A. The 37-nt deletion in LASV NP ExoN-

(**1**) Mis-incorporation/stop

```
5'-UAAAUGGACGCCCCCGUGACA*
   |||||||||||||||||||||
3'-AUUUACCUGCGGGGGCACUGg.........gggacugUCCCAGAGUA
```

Site I **Site I'**

(**2**) Re-align/resume

```
5'-UAAAUGGACGCCCCCGUGACA-------->
                  ||||||| |
3'-AUUUACCUGCGGGGGCACUGg........gccccgggacugUUCCCAGAGUA
```

B. The 231-nt deletion in LASV NP ExoN-

(**1**) Mis-incorporation/stop

NP **Site II'** **Site II** IGR

```
SagRNA 5'-AAAGACUUAUGCCACaug.........gGUCACGGGGGCCCUGACAAGGGUC
                                      ||||||||||||||||||||||
                                     *ACAGUGCCCCCGGGACUGUUCCCAG-5'
```

(**2**) Re-align/resume

```
5'-AAAGACUUAUGCCACaug.........gGUCACGGGGGCCCUGACAAGGGUC
              ||||||
<-----ACAGUGCCCCCGGGACUGUUCCCAG-5'
```